Article

Mechanisms of Antibiotic Resistance: QM/MM Modeling of the Acylation Reaction of a Class A β-Lactamase with Benzylpenicillin

Johannes C. Hermann, Christian Hensen, Lars Ridder, Adrian J. Mulholland, and Hans-Dieter Hltje

J. Am. Chem. Soc., **2005**, 127 (12), 4454-4465• DOI: 10.1021/ja044210d • Publication Date (Web): 08 March 2005

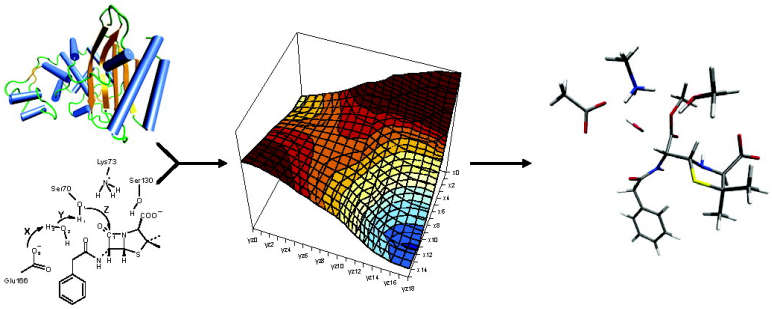

More About This Article

Additional resources and features associated with this article are available within the HTML version:

- Supporting Information
- Links to the 11 articles that cite this article, as of the time of this article download
- Access to high resolution figures
- Links to articles and content related to this article
- Copyright permission to reproduce figures and/or text from this article

View the Full Text HTML

J|A|C|S
ARTICLES
Published on Web 03/08/2005

Mechanisms of Antibiotic Resistance: QM/MM Modeling of the Acylation Reaction of a Class A β-Lactamase with Benzylpenicillin

Johannes C. Hermann,[†,§] Christian Hensen,[†] Lars Ridder,[‡,§] Adrian J. Mulholland,*[,§] and Hans-Dieter Höltje*[,†]

Contribution from the Institut für Pharmazeutische Chemie, Heinrich-Heine Universität Düsseldorf, Universitätsstrasse 1, 40225 Düsseldorf, Germany, Molecular Design & Informatics, N.V. Organon, P.O. Box 20, 5340 BH Oss, The Netherlands, and School of Chemistry, University of Bristol, Bristol BS8 1TS, U.K.

Received September 23, 2004; E-mail: adrian.mulholland@bristol.ac.uk; hoeltje@pharm.uni-duesseldorf.de

Abstract: Understanding the mechanisms by which β-lactamases destroy β-lactam antibiotics is potentially vital in developing effective therapies to overcome bacterial antibiotic resistance. Class A β-lactamases are the most important and common type of these enzymes. A key process in the reaction mechanism of class A β-lactamases is the acylation of the active site serine by the antibiotic. We have modeled the complete mechanism of acylation with benzylpenicillin, using a combined quantum mechanical and molecular mechanical (QM/MM) method (B3LYP/6-31G+(d)//AM1-CHARMM22). All active site residues directly involved in the reaction, and the substrate, were treated at the QM level, with reaction energies calculated at the hybrid density functional (B3LYP/6-31+G(d)) level. Structures and interactions with the protein were modeled by the AM1-CHARMM22 QM/MM approach. Alternative reaction coordinates and mechanisms have been tested by calculating a number of potential energy surfaces for each step of the acylation mechanism. The results support a mechanism in which Glu166 acts as the general base. Glu166 deprotonates an intervening conserved water molecule, which in turn activates Ser70 for nucleophilic attack on the antibiotic. This formation of the tetrahedral intermediate is calculated to have the highest barrier of the chemical steps in acylation. Subsequently, the acylenzyme is formed with Ser130 as the proton donor to the antibiotic thiazolidine ring, and Lys73 as a proton shuttle residue. The presented mechanism is both structurally and energetically consistent with experimental data. The QM/MM energy barrier (B3LYP/6-31G+(d)//AM1-CHARMM22) for the enzymatic reaction of 9 kcal mol^{-1} is consistent with the experimental activation energy of about 12 kcal mol^{-1}. The effects of essential catalytic residues have been investigated by decomposition analysis. The results demonstrate the importance of the "oxyanion hole" in stabilizing the transition state and the tetrahedral intermediate. In addition, Asn132 and a number of charged residues in the active site have been identified as being central to the stabilizing effect of the enzyme. These results will be potentially useful in the development of stable β-lactam antibiotics and for the design of new inhibitors.

Introduction

β-Lactamases are bacterial enzymes responsible for most resistance against β-lactam antibiotics. They present a serious and growing threat to the efficacy of antibacterial chemotherapy and thus pose a major challenge to human health.[1−3] These defensive enzymes, prevalent in nearly every pathogenic bacterial strain, hydrolyze the β-lactam ring and release the cleaved, inactive antibiotics. Therefore, the major focus for the development of new β-lactam antibiotics (besides specific inhibitor design) is to improve the stability of the compounds against β-lactamases. Knowledge about the molecular mechanism of action of these enzymes should be very helpful for these purposes. Unfortunately, the reaction mechanism has not been clarified to date: a number of different proposals have been made.[4−6]

The enzyme family of β-lactamases is divided into four classes,[7] according to their sequence relationships. Those of class B are zinc-dependent proteins, whereas classes A, C, D and penicillin-binding-proteins (PBPs) are active site serine enzymes (β-lactamases are believed to have evolved in bacteria from PBPs, the natural targets of β-lactam antibiotics[8,9]). The most common are class A β-lactamases, such as TEM1 from *E. coli*, on which we focus here.[10] We have modeled the acylation

[†] Heinrich-Heine Universität Düsseldorf.
[‡] Molecular Design & Informatics.
[§] University of Bristol.

(1) Neu, H. C. *Science* **1992**, *257*, 1064−1073.
(2) Cohen, M. L. *Science* **1992**, *257*, 1050−1055.
(3) Davies, J. *Science* **1994**, *264*, 375−382.
(4) Matagne, A.; Lamotte-Brasseur, J.; Frère, J.-M. *Biochem. J.* **1998**, *330*, 581−598.
(5) Massova, I.; Kollman, A. P. *J. Comput. Chem.* **2002**, *23*, 1559−1576.
(6) Díaz, N.; Sordo, T. L.; Merz, K. M., Jr.; Suárez, D. *J. Am. Chem. Soc.* **2003**, *125*, 672−684.
(7) Ambler, R. P. *Philos. Trans. R. Soc. London, Ser. B* **1980**, *289*, 321−331.
(8) Massova, I.; Mobashery, S. *Antimicrob. Agents Chemother.* **1998**, *42*, 1−17.
(9) Matagne, A.; Misselyn-Bauduin, A.-M.; Joris, B.; Erpicum, T.; Granier, B.; Frère, J.-M. *Biochem. J.* **1990**, *265*, 131−146.

10.1021/ja044210d CCC: $30.25

mechanism of the TEM1 enzyme by the most comprehensive QM/MM calculations to date, with a large, realistic protein model incorporating the potentially vital effects of the protein environment (unlike previous small model studies[5,11]). Energies have been corrected with quantum chemical calculations at high levels (hybrid density functional theory) that go well beyond our previous semiempirical QM/MM investigations.[12] The potential energy surfaces (PESs) presented here should provide a reliable description of the reaction energies.

In class A β-lactamases, Ser70 attacks the labile lactam bond (the standard amino acid numbering scheme for β-lactamases of Ambler et al. is used[13]). Lys73 is known to be catalytically important[14] (see below) and forms hydrogen bonds to Ser70, Ser130, Asn132, and Glu166.[4,15] A special feature of the active site is a structurally conserved water that is hydrogen bonded to Ser70, Glu166, and Asn170. All of these residues are likely to be involved in catalysis, but the molecular mechanism has been uncertain, as discussed below.

The reaction mechanism of class A β-lactamases consists of two main steps. The first step is acylation of Ser70 by the β-lactam antibiotic; the second is hydrolysis of the resulting ester, the acylenzyme intermediate. The deacylation mechanism, in which the conserved water molecule is activated by Glu166 to hydrolyze the acylenzyme intermediate, is widely accepted.[16] In contrast, the acylation mechanism is the subject of debate. The general base that activates Ser70 is not known. Various acylation mechanisms have been proposed, involving different candidates. One proposes Lys73 as the base.[16] The unusual neutral state of Lys73 required for this mechanism was suggested to be favored by its electrostatic environment in the active site and by substrate effects.[17,18] However, several theoretical and experimental investigations indicate that Lys73 is more likely to be protonated under physiological conditions and consequently cannot act as the base.[19−21] Furthermore, we have performed molecular dynamics simulations which suggest that Lys73 exists in a protonated state, based on analysis of the stability of the hydrogen-bond network in the active site and RMS deviations of conserved residues. In particular, the conserved water molecule, unambiguously needed for deacylation, did not remain in its position in the active site when Lys73 was treated as neutral.[22] Similarly, Díaz et al. concluded from their molecular dynamics simulations that Lys73 is unlikely to be the base.[6] This mechanism (Lys73 as the base) has been modeled in a QM/MM study by Pitarch et al.[23] Another mechanism has been proposed in a QM/MM study by Díaz et al. involving the substrate's carboxylate group as the base.[24] However, the latest experimental data make both of these mechanisms appear unlikely (see below).

An alternative proposal involves Glu166 as the base.[25,26] This mechanism is supported by our previous QM/MM calculations[12] and by two published ultrahigh resolution X-ray structures of class A β-lactamases. In one of these structures, with a transition state analogue bound to the active site, Glu166 is protonated. The other shows Ser70 hydrogen bonded to the bridging water molecule. Both structures therefore support a mechanism in which Glu166 acts as the general base.[27,28] Experiments show that both Glu166 and Lys73 are essential for efficient acylation.[18,25,29−32] E166-mutants (and K73 mutants) are acylated but at a drastically reduced rate. The E166 mutants also lose the ability to hydrolyze the acylenzyme intermediate. However, the glutamate seemed unlikely to act as the general base because it is too far away (3−4 Å) to abstract a proton directly from Ser70. Molecular dynamics simulations indicated that the loop containing Glu166 is very flexible, suggesting that a direct abstraction of the proton might be possible.[33] However, it is more likely that a catalytic water molecule acts as a relay station,[12,26] analogous to the deacylation reaction.

We show here, by QM/MM calculations with high-level energy corrections, that a mechanism involving Glu166 as the general base deprotonating the conserved water molecule is energetically and structurally reasonable, and consistent with experimental data. The full acylation reaction is modeled here for the first time with all reaction processes included and (in contrast to some other computational studies of this reaction[23]) with Lys73 in its physiological, protonated state.[21,27,28] We have calculated potential energy surfaces for the reaction, and the degree of concertedness has been investigated. We have analyzed the contribution of individual amino acids to the reaction energetics. The results reveal new details of the reaction mechanism, in particular structures of key species along the reaction paths (e.g., transition states and intermediates), which may help in the design of new antibiotics, more resistant to breakdown by β-lactamases.

Methods

Application of the QM/MM Potential. We applied the AM1-CHARMM22 QM/MM method for modeling the reaction.[34] This has been used successfully in a number previous studies of enzyme

(10) Massova, I.; Mobashery, S. *Curr. Pharm. Des.* **1998**, *5*, 929−937.
(11) Wladkowski, B. D.; Chenoweth, S. A.; Sanders, J.; Krauss, M.; Stevens, W. J. *J. Am. Chem. Soc.* **1997**, *119*, 6423−6431.
(12) Hermann, J. C.; Ridder, L.; Mulholland, A. J.; Höltje, H.-D. *J. Am. Chem. Soc.* **2003**, *125*, 9590−9591.
(13) Ambler, R. P.; Coulson, A. F. W.; Frère, J.-M.; Ghuysen, J.-M.; Joris, B.; Forsman, M.; Levesque, R. C.; Tiraby, G.; Waley, S. G. *Biochem. J.* **1991**, *276*, 269−272.
(14) Lietz, E. J.; Truher, D. K.; Hokenson, M. J.; Fink, A. L. *Biochemistry* **2000**, *39*, 4971−4981.
(15) Jelsch, C.; Mourey, L.; Masson, J. M.; Samama, J. P. *Proteins* **1993**, *16*, 364−383.
(16) Oefner, C.; Winkler, F. K. *Nature* **1990**, *343*, 284−288.
(17) Swarén, P.; Maveyraud, L.; Guillet, V.; Masson, J.-M.; Mourey, L.; Samama, J.-M. *Structure* **1995**, *3*, 603−613.
(18) Strynadka, N. C. J.; Adachi, H.; Jensen, S. E.; Johns, K.; Sielecki, A.; Betzel, C.; Sutoh, K.; James, M. N. G. *Nature* **1992**, *359*, 700−705.
(19) Lamotte-Brasseur, J.; Wade, R.; Raquet, X. *Protein Sci.* **1999**, *8*, 404−409.
(20) Raquet, X.; Lounnas, V.; Lamotte-Brasseur, J.; Frère, J.-M.; Wade, R. *Biophys. J.* **1997**, *73*, 2416−2426.
(21) Damblon, C.; Raquet, X.; Lian, L.-Y.; Lamotte-Brasseur, J.; Fonze, E.; Charlier, P.; Gordon, C. K. R.; Frère, J.-M. *Proc. Natl. Acad. Sci. U.S.A.* **1996**, *93*, 1747−1752.
(22) Hermann, J. C. Thesis, Cuvillier, Göttingen, 2004.
(23) Pitarch, J.; Pascal-Ahuir, J.-L.; Silla, E.; Tunón, I. *J. Chem. Soc., Perkin Trans.2* **2000**, 761−767.
(24) Díaz, N.; Suárez, D.; Sordo, T. L.; Merz, K. M., Jr. *J. Phys. Chem. B* **2001**, *105*, 11302−11313.
(25) Gibson, R. M.; Christensen, H.; Waley, S. G. *Biochem. J.* **1990**, *272*, 613−619.
(26) Lamotte-Brasseur, J.; Dive, G.; Dideberg, O.; Charlier, P.; Frère, J.-M.; Ghuysen, J.-M. *Biochem. J.* **1991**, *279*, 213−221.
(27) Minasov, G.; Wang, X.; Shoichet, B. K. *J. Am. Chem. Soc.* **2002**, *124*, 5333−5340.
(28) Nukaga, M.; Mayama, K.; Hujer, A.; Bonomo, R. A.; Knox, J. R. *J. Mol. Biol.* **2003**, *328*, 289−301.
(29) Guillaume, G.; Vanhove, M.; Lamotte-Brasseur, J.; Ledent, P.; Jamin, M.; Joris, B.; Frère, J.-M. *J. Biol. Chem.* **1997**, *272*, 5438−5444.
(30) Escobar, W. A.; Tan, A. K.; Fink, A. L. *Biochemistry* **1991**, *30*, 10783−10787.
(31) Adachi, H.; Ohta, T.; Matsuzawa, H. *J. Biol. Chem.* **1991**, *266*, 3186−3191.
(32) Lietz, E. J.; Truher, D. K.; Hokenson, M. J.; Fink, A. L. *Biochemistry* **2000**, *39*, 4971−4981.
(33) Vijayakumar, S.; Ravishanker, G.; Pratt, R. F.; Beveridge, D. L. *J. Am. Chem. Soc.* **1995**, *117*, 1722−1730.
(34) Field, M. J.; Bash, P. A.; Karplus, M. *J. Comput. Chem.* **1990**, *11*, 700−733.

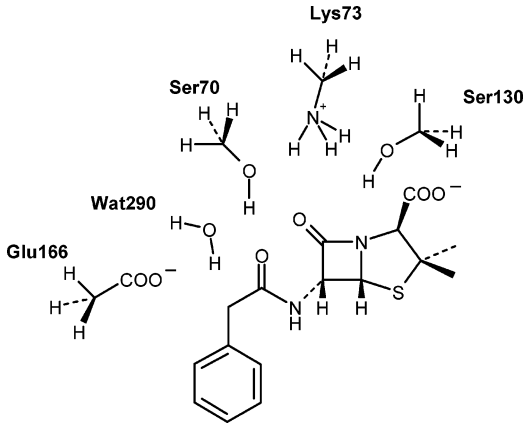

Figure 1. The QM-region of the QM/MM model. The covalent bonds between the amino acid side chains and the rest of the protein are replaced by bonds to QM hydrogen "link" atoms (MM covalent bonded terms are retained).

mechanisms.[35−37] A large quantum mechanical region of 70 atoms in total (34 heavy atoms, see Figure 1) was defined including the catalytic water (Wat290), the substrate benzylpenicillin, and parts of the side chains of Ser70, Lys73, Ser130, and Glu166. The QM-region had a total charge of −1*e*. Four hydrogen "link atoms" were introduced to saturate the shells of QM-atoms covalently bonded to MM-atoms. In contrast to the standard "QQ"-type link atom,[34] the applied ("HQ") link atoms do "feel" the MM-atom point charges, which has been shown to be more appropriate.[38] For the QM-atoms, standard van der Waals parameters of the CHARMM22 force field[39] were used. For reasons of computational feasibility, the large QM region of the model system was described by the semiempirical AM1 Hamiltonian during all QM/MM geometry optimization steps.[40,41] We have tested the suitability of AM1 for the calculation of β-lactam geometries by comparisons with higher level calculated geometries and with the crystal structure[42] (see Supporting Information). Subsequently, the calculated AM1-CHARMM22 energetics were corrected by higher level hybrid density functional theory (DFT) calculations as detailed below.

All of the remaining atoms (3216 atoms in total, including 51 crystal water molecules, and 174 added water molecules) were handled at the molecular mechanical level, using the CHARMM22 force field. For the water molecules, the CHARMM variant of the TIP3P model was used.[39,43]

Construction of a Model of TEM1 β-Lactamase. The high-resolution crystal structure of the benzylpenicillin acylated E166N mutant TEM1 β-lactamase from *Escherichia Coli* (PDB[44] entry code 1FQG[18]) was chosen as the starting geometry to perform calculations with the QM/MM module[34] of the CHARMM molecular mechanics package (version 27b2).[45] First, the E166N mutation was mutated (in silico) back to glutamate to generate a functional (wild type) active site. For this, we used the internal coordinates of the Glu166 side chain from a wild-type TEM1 crystal structure (PDB entry code 1BTL[15]). A model of the reactive substrate complex was then generated following procedures similar to previous QM/MM investigations of other enzymes.[35,46] Hydrogens were added using the HBUILD routine[47] in CHARMM. Following the N166E back mutation, only the position of the conserved water molecule had to be optimized to obtain the wild-type hydrogen-bond network. Other residues of the mutant active site do not differ in their orientation in comparison to the wild type (hydrogen bonds are defined throughout the paper by the default CHARMM cutoffs).[18] An initial MM optimization of all hydrogen atoms was performed. The system was then solvated by superimposing a 26 Å (previously equilibrated) water sphere centered on the reaction center (the oxygen of the Ser70 hydroxyl-group), and deleting any water molecules with its oxygen within 2.6 Å of another heavy atom. The enzyme was then truncated by deleting every residue and water molecule that did not have at least one heavy atom within 18 Å of the reaction center. After equilibration by 10 ps of (MM) Langevin dynamics (at 300 K) for all water molecules (all other atoms fixed), the solvation procedure (sphere addition, deletion, and equilibration) was repeated, giving in total 51 crystal and 175 added water molecules. Finally, the positions of the water molecules were optimized by 4000 steps of steepest descent minimization and 882 steps of adopted basis Newton−Raphson (ABNR) energy minimization with MM (in MM minimizations, standard CHARMM22 charges were used for atoms of the QM-region, which was fixed).[48] The crystal structure was then relaxed by 500 steps of steepest descent QM/MM minimization, applying harmonic restraints to heavy atoms of the backbone and side chains (50 and 25 kcal mol^{-1} Å^{-2}, respectively). To get the final model (representing the acylenzyme intermediate), the energy of the system was minimized (by AM1-CHARMM22 QM/MM) to achieve a gradient tolerance of 0.01 kcal mol^{-1} Å^{-1}, which took 1000 steps of steepest descent and 1839 steps of ABNR-minimization. As for all subsequent calculations, a nonbonded cutoff of 12 Å was applied using a group-based switching function to scale the electrostatic interactions smoothly down over a 8−12 Å distance. All QM-atoms (see below) were defined as one group to ensure that the MM charges were treated consistently in the Hamiltonian for the QM-atoms. All heavy atoms further than 14 Å from the reaction center were harmonically restrained to their relaxed crystal coordinates with force constants based on model average *B*-factors.[49]

Calculation of Potential Energy Surfaces. One or more reaction coordinates were defined for every reaction step and restrained sequentially to move the system along a given reaction path. The distance-dependent reaction coordinate restraints were applied using the RESD command of CHARMM.[50] The value for each reaction coordinate was defined by the subtraction of one interatomic distance from another for three atoms (e.g., for a proton transfer, the distance between the accepting oxygen and the moving hydrogen was subtracted from the distance between that hydrogen and the donating oxygen). When a third distance was included in one reaction coordinate, additional restraints had to be applied, which were only active when a given distance fell below or exceeded a given limit during a geometry optimization. When a reaction coordinate is defined as a linear combination of more than two distances, the constrained system has more than one degree of freedom, which makes it often difficult to force the system to cross an energy barrier (and resulting in "unrealistic jumps" during a single optimization). In these cases, additional restraints that allow specific distances to change only in a certain direction were

(35) Ridder, L.; Mulholland, A. J.; Rietjens, M. C. M. I.; Vervoort, J. *J. Am. Chem. Soc*. **2000**, *122*, 8728−8738.
(36) Mulholland, A. J.; Richards, W. G. *Proteins* **1997**, *27*, 9−25.
(37) Gao, J.; Truhlar, D. G. *Annu. Rev. Phys. Chem.* **2002**, *53*, 467−505.
(38) Reuter, N.; Dejaegere, A.; Maigret, B.; Karplus, M. *J. Phys. Chem. A* **2000**, *104*, 1720−1735.
(39) MacKerell, A. D.; Bashford, D.; Bellot, M.; Dunbrack, R. L.; Evanseck, J. D.; Field, M. J.; Fischer, S.; Gao, J.; Guo, J.; Ha, S.; Joseph-McCarthy, D.; Kuchnir, L.; Kuczera, K.; Lau, F. T. K.; Mattos, C.; Michnick, S.; Ngo, T.; Nguyen, D. T.; Prodhom, B.; Reiher, W. E.; Roux, B.; Schlenkrich, M.; Smith, J. C.; Stote, R.; Straub, J.; Watanabe, M.; Wiorkiewicz-Kuczera, J.; Yin, D.; Karplus, M. *J. Phys. Chem. B* **1998**, *102*, 3586−3616.
(40) Dewar, M. J. S.; Zoebisch, E. G.; Healy, E. F.; Stewart, J. J. P. *J. Am. Chem. Soc.* **1985**, *107*, 3902−3909.
(41) Dewar, M. J. S.; Zoebisch, E. G. *J. Mol. Struct. (THEOCHEM)* **1988**, *180*, 1−21.
(42) Dexter, D. D.; van der Veen, J. M. *J. Chem. Soc., Perkin Trans.1* **1978**, *3*, 3185−3190.
(43) Jorgensen, W. L.; Chandrasekhar, J.; Madura, J. D.; Impey, R. W.; Klein, M. L. *J. Chem. Phys.* **1983**, *79*, 926−935.
(44) Berman, H. M. *Nucleic Acids Res.* **2000**, *28*, 235−242.
(45) Brooks, B. R.; Bruccoleri, R. E.; Olafson, B. D.; States, D. J.; Swaminathan, S.; Karplus, M. *J. Comput. Chem*. **1983**, *4*, 187−217.
(46) Ridder, L.; Rietjens, I. M. C. M.; Vervoort, J.; Mulholland, A. J. *J. Am. Chem. Soc*. **2002**, *124*, 9926−9936.
(47) Brunger, A. T.; Karplus, M. *Proteins* **1988**, *4*, 148−156.
(48) Boyd, R. H. *J. Chem. Phys.* **1968**, *19*, 2574−2583.
(49) Brooks, C. L., III; Karplus, M. *J. Mol. Biol.* **1989**, *208*, 159−181.
(50) Eurenius, K. P.; Chatfield, D. C.; Brooks, B. R.; Hodoscek, M. *Int. J. Quantum Chem.* **1996**, *60*, 1189−1200.

applied to ensure the overall progress of a reaction (details of individual reaction coordinates and restraints are given below). A force constant of $k = 5000$ kcal mol^{-1} Å^{-2} was used to restrain all of the defined coordinates. The values for the restrained distances were increased or decreased continuously to force the system across the barrier of a particular reaction step. The step size was decreased around the approximate transition states to scan the surface more precisely at these points. Energy minimizations (by ABNR) of all structures were performed to a gradient tolerance of 0.01 kcal mol^{-1} Å^{-1}. The structures of energy minima (i.e., stable structures) were determined more precisely by performing additional geometry optimizations with none of the reaction coordinates restrained. The final energy of a structure (as indicated on the potential energy surfaces, for example) was obtained by single-point energy calculations where the energy contribution derived from any restraints was left out. The potential energy surfaces provide insight into mechanistic features such as the identification of transition states and intermediates, and whether multiple reactions occur stepwise or concerted. However, it should be remembered that the PES does not represent factors such as zero-point energy, entropic effects, and hydrogen tunneling effects that may affect fine details and will alter effective barriers to reaction. Furthermore, only one representative conformation of the enzyme is considered (based on the crystal structure). All active site residues are free to move and adapt to changes during the reaction, but large-scale changes in the protein conformation cannot occur. However, calculations using different local minima as starting geometries gave similar results.[22] The overall conclusions drawn here regarding the mechanism are not sensitive to the structural model.

Energy Corrections. High-level QM/MM molecular modeling approaches (e.g., based on ab initio or density functional theory[51]) are currently too computationally expensive to calculate several potential energy surfaces with a large QM-region as required for modeling the reaction here. To obtain energies as accurately as possible, the QM/MM potential energy surfaces were corrected with higher level B3LYP energies in the following way. The geometries of the QM-atoms of every structure were isolated, and vacuum single-point energy calculations were performed at the AM1 and B3LYP/6-31G+(d) levels, respectively (for DFT calculations, the Jaguar program was used[52]). Thus, for the results presented here, approximately 550 DFT calculations were needed (i.e., around 275 per surface, in addition to the AM1 vacuum single point, and the QM/MM calculations). The corrected energy values were obtained by subtracting from the total QM/MM energy the AM1 energy of the isolated QM-region and adding the B3LYP energy. The B3LYP corrected potential energy surfaces consist therefore of the B3LYP vacuum energy, of the CHARMM22 MM energy, and of the AM1/CHARMM22 QM/MM interaction energy, which has been shown to be of good quality generally.[35,53,54] Interactions with the enzyme should therefore be described reasonably. The accuracy of results of B3LYP/6-31G+(d) calculations on AM1 optimized structures has been found to be significantly better than AM1 energies.[55] Similar energy corrections have been performed in a QM/MM study of another enzyme, chorismate mutase, where it was shown that the corrected energies (which are designated as B3LYP/6-31G+(d)//AM1-CHARMM22) give results comparable to those of full ab initio QM/MM-calculations.[53,56]

Amino Acid Decomposition Analysis. Important structures of the acylation reaction were investigated in detail by decomposition of the protein environment using a procedure similar to that described in ref 36. All MM residues were removed in decreasing order of their center of mass distance to the center of the simulation system (which was based on the initial position of the hydroxylic oxygen of Ser70). After every deletion, the QM/MM interaction energy (AM1-CHARMM22) was recalculated. The interaction energy consists of van der Waals energy and of the dominating electrostatic energy. This method does not (and is not intended to) provide energies comparable to results derived from mutation experiments. Nevertheless, the observable calculated change in interaction energy gives an estimate of the contribution of an amino acid to the stabilization of the structure. This can help to identify vital interactions of the enzyme and the substrate or quantum mechanically treated active site residues (i.e., the MM-region and the QM-region).[35,36] Additional insight comes from consideration of changes in charge distribution during the reaction. The use of a quantum mechanical method allows changes in electronic structure during the reaction to be studied. Therefore, a Mulliken population analysis[57] (AM1-CHARMM22 QM/MM, i.e., including the polarization of the QM atoms by the MM system) was performed for the QM-atoms of the investigated structures. This provides an indication of the most important changes in electronic structure during the reaction.

Scheme 1. Individual Reaction Processes Involved in the First Modeled Step of the Acylation Mechanism of Class A β-Lactamases: The Nucleophilic Attack and Formation of the Tetrahedral Intermediate

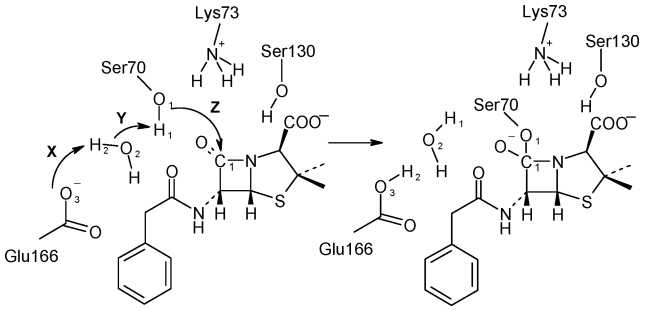

Results and Discussion

1. Reaction Path Calculations. The starting structure represents the acylenzyme after nucleophilic attack of Ser70 has taken place. Therefore, we modeled the reaction initially in the backward direction (i.e., to generate the substrate). Subsequently, calculations were performed in the forward direction to test that the results were consistent in both directions. Similar results were obtained in both cases. A number of alternative possible mechanisms based on Glu166 as the general base were investigated.[22] These various mechanisms were tested by calculating different potential energy surfaces. Only one was found to be consistent with experimental data and energetically and structurally reasonable. We present here the results for that mechanism, modeled in the forward direction from the Michaelis complex to the acylenzyme.

Acylation Step 1: Formation of the Tetrahedral Intermediate. In our model, the first reaction step of the acylation consists of three events (see Scheme 1). A proton is abstracted from Ser70 (**Y**), and, via a bridging water, a second proton is transferred to the general base Glu166 (**X**). The deprotonated Ser70 attacks the carbonyl group of the β-lactam ring (**Z**). The barrier for this whole process is the highest barrier along the reaction path for acylation, as discussed below: formation of the tetrahedral intermediate is likely to be the rate-determining step overall.

(51) Mulholland, A. J.; Lyne, P. D.; Karplus, M. *J. Am. Chem. Soc.* **2000**, *122*, 534−535.
(52) *Jaguar 4.1*; Schrödinger, Inc.: Portland, OR, 1991−2000.
(53) Ridder, L.; Harvey, J. N.; Rietjens, I. M. C. M.; Vervoort, J.; Mulholland, A. J. *J. Phys. Chem. B* **2003**, *107*, 2118−2126.
(54) Ridder, L.; Mulholland, A. J.; Vervoort, J.; Rietjens, I. M. C. M. *J. Am. Chem. Soc.* **1998**, *120*, 7641−7642.
(55) Foreman, J. B.; Frisch, A. E. High Accuracy Energy Models. *Exploring Chemistry with Electronic Structure Methods*, 2nd ed.; Gaussian, Inc.: Pittsburgh, PA, 1996; pp 155−161.
(56) Ranaghan, K. E.; Ridder, L.; Szefczyk, B.; Sokalski, W. A.; Hermann, J. C.; Mulholland, A. J. *Mol. Phys.* **2003**, *101*, 2695−2714.
(57) Mulliken, R. S. *J. Chem. Phys.* **1955**, *23*, 1833−1844.

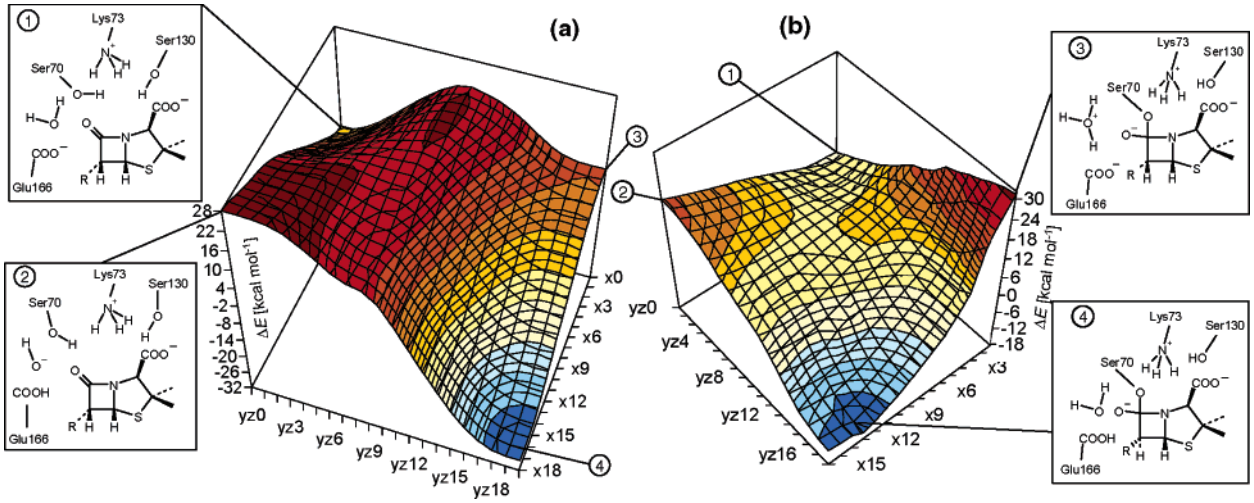

Figure 2. QM/MM potential energy surfaces for the reaction coordinates R_{RX} and R_{YZ}. (a) AM1-CHARMM22-energies, (b) B3LYP/6-31G+(d)//AM1-CHARMM22-energies. (1) is the Michaelis complex; (2) and (3) are unstable structures; and (4) is the tetrahedral intermediate.

Our previous investigations indicated that the events **Y** and **Z** happen in a concerted way, and we found that proton transfer **X** is also concerted to some degree with these processes.[12] Therefore, all three events were included in the calculation of the potential energy surface for this step. The first reaction coordinate, R_X, modeled proton transfer **X** (see Scheme 1: $R_X = d[O_2{:}H_2] - d[O_3{:}H_2]$, increments 0.1 Å), whereas **Y** and **Z** were merged in one reaction coordinate ($R_{YZ} = d[O_1{:}H_1] - d[O_2{:}H_1] - d[C_1{:}O_1]$, increments 0.15 Å). The AM1-CHARMM22 and B3LYP/6-31G+(d)//AM1-CHARMM22 surfaces are shown in Figure 2a and b, respectively, where the Michaelis substrate complex is represented by geometry [x0;yz0] (1). The change of the energy during the protonation of Glu166 can be observed along reaction coordinate R_X. The definition of R_{YZ} allowed both restrained processes (Ser70 activation and nucleophilic attack, **Y** and **Z**) the freedom to change for every value of R_X.

We discuss first the AM1-CHARMM22 surface; this is qualitatively similar in many respects to the higher level surface (which is discussed below), but there are some important differences. The lowest energy path on the AM1-CHARMM22 surface that connects the Michaelis complex with the tetrahedral intermediate goes approximately diagonally through the middle of the surface crossing the barrier at the coordinates [x7;yz9], indicating that all reaction processes are concerted. In the transition state, the two proton transfers **X** and **Y** are occurring (see Figure 3). The proton that is transferred for activation (see Scheme 1, H_1, **Y**) is equidistant (1.2 Å) between the donating oxygen atom of Ser70 and the accepting oxygen of the water molecule. Transfer **Y** is apparently a little more advanced in the TS. The length of the forming bond between the oxygen of Glu66 and the former water hydrogen is shorter (1.1 Å). The distance between the Ser70 oxygen and the substrate carbonyl carbon is significantly decreased from 2.5 Å in the Michaelis complex to 2 Å at the transition state. The carbonyl group is not planar at the transition state, indicating the nucleophilic attack is in progress. The AM1-CHARMM22 surface suggests that a sequential mechanism of proton transfer **X** with **YZ** could occur. This is unlikely based on the higher level results (see below) and a consequence of the previously observed artificial stability predicted by AM1 for structures with a hydroxonium ion in the active site (i.e., low values for R_X and high values for R_{YZ}).[12] Further evidence that the concerted mechanism is more likely came from the observation of spontaneous concerted reactions in various other calculations, in which restraints were not applied to all of the coordinates considered here (e.g., when initially only the proton transfers **X** and **Y** were restrained, the minimizations at a specific stage of the reaction optimized toward structures in which the nucleophilic attack (**Z**) had occurred spontaneously).[22] Similar behavior was observed when other combinations of restraints were applied.

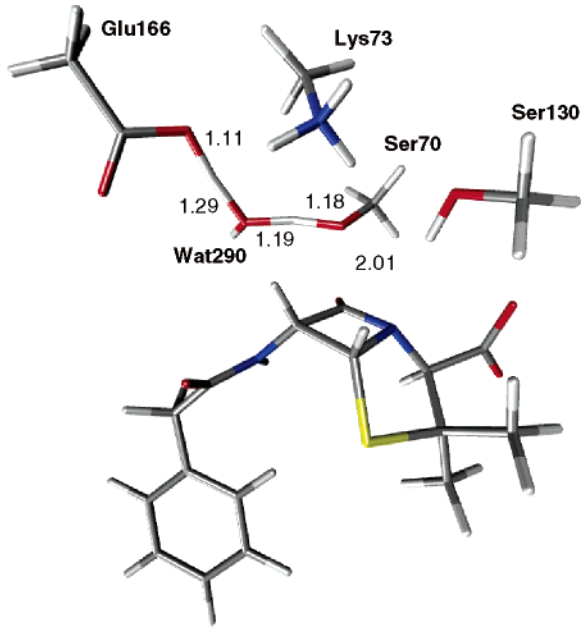

Figure 3. Structure of the transition state of the first acylation step, showing the QM atoms only, at the AM1-CHARMM22 level (point [x7;yz9] in Figure 2). The structure at the B3LYP//AM1-CHARMM22 level ([x6;yz7] in Figure 2) is very similar. Distances are given in angstroms throughout. Figures were generated using VMD.[76]

The B3LYP/6-31G+(d)//AM1-CHARMM22 surface even more clearly supports a concerted reaction mechanism, because the lowest energy path goes approximately through the middle of the surface. Geometries containing hydroxonium ions are high in energy (low values for R_X and high values for R_{YZ}). Pathways involving these structures (as suggested by AM1) are therefore very unlikely. The transition state ([x6;yz7]) is a little different,

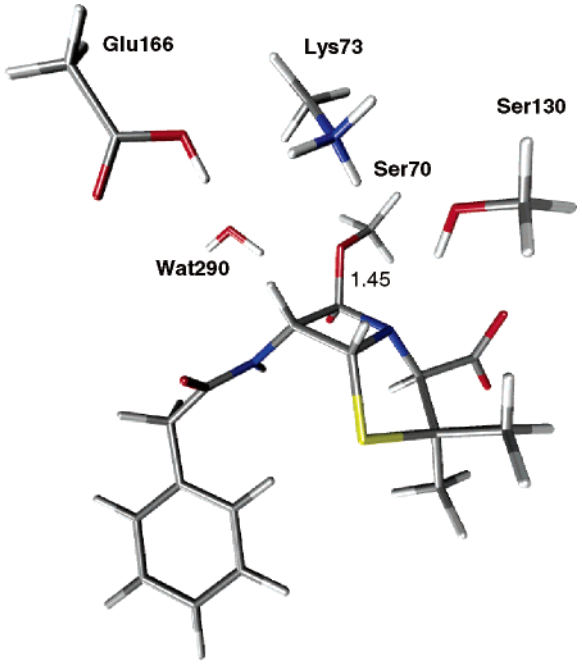

Figure 4. Structure of the tetrahedral intermediate of the first acylation step, showing the QM atoms only (AM1-CHARMM22; point [x17;yz19] in Figure 2). The Ser70 O−lactam C distance is shown in angstroms.

showing slightly less activation of Ser70 as compared to that predicted at the AM1-CHARMM22 level: the proton of Ser70 is more tightly bound (O_1-H_1 distance of 1.11 Å). The progress of the other proton transfer (**X**) is similar to the AM1-CHARMM22 result, with O−H distances of 1.1−1.3 Å. Both transition state geometries suggest that the barrier-determining process of the acylation is the activation (deprotonation) of Ser70.

The structure of the tetrahedral intermediate (i.e., the position of the corresponding minimum, see Figure 2 ([x12;yz17])), is also slightly different from the AM1-CHARMM22 result ([x17;yz19]). This is probably a consequence of the different positions of the water molecule caused by the longer hydrogen-bond lengths preferred by AM1 as compared to B3LYP.[58,59] However, the water molecule is not involved in acylation after proton transfer, and so its exact position is not as crucial as in the first event. Both methods show the expected tetrahedral conformation in the intermediate. The former carbonyl oxygen bond points roughly in the opposite direction of the now covalently bound Ser70 oxygen of the newly formed ester bond, with a C_1-O_1 bond length of 1.45 Å (see Scheme 1, Figure 4).

As expected, the calculated barriers for the first reaction step differ significantly between the two methods. AM1-CHARMM22 gives a barrier height of 19.6 kcal mol^{-1}, considerably higher than the barrier at the B3LYP/6-31G+(d)//AM1-CHARMM22 level (8.7 kcal mol^{-1}). Semiempirical methods such as AM1 are known to overestimate reaction barriers in many cases.[58] Furthermore, the geometry of the transition state involves two proton transfers in hydrogen bonds. B3LYP gives better results for hydrogen bonds than AM1 but tends to overestimate their stability somewhat,[59,60] while it often underestimates barriers for proton transfers.[61,62] The barrier predicted at the B3LYP/6-31G+(d)//AM1-CHARMM22 level may therefore be somewhat too low, although it is likely to be considerably more realistic than the AM1-CHARMM22 result.

Scheme 2. Individual Modeled Reaction Processes Involved in the Second Step of the Proposed Acylation Mechanism of Class A β-Lactamases: Formation of the Acylenzyme from the Tetrahedral Intermediate

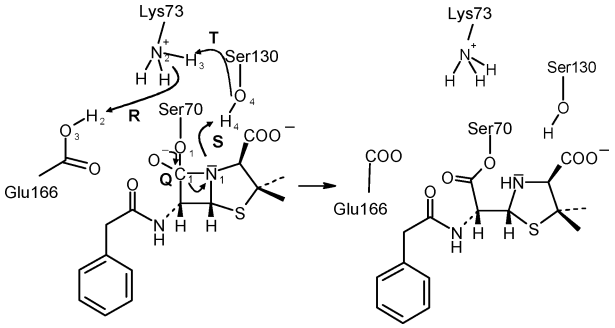

Acylation Step 2. Formation of the Acylenzyme. The subsequent formation of the acylenzyme from the tetrahedral intermediate is also a complex multiproton-transfer process. This completes the breakdown of the lactam bond (see Scheme 2, step **Q**). The calculations support a mechanism in which the leaving thiazolidine nitrogen (N_1) is protonated by Ser130 (step **S**). Ser130 is reprotonated by Glu166 via Lys73 as a relay station (steps **R** and **T**). At the AM1-CHARMM22 level, only one of the various possible combinations of reaction coordinates resulted in a continuous potential energy surface. This surface was calculated starting from the tetrahedral intermediate using two reaction coordinates that represented steps **Q** (see Scheme 2: $R_Q = d[C_1{:}N_1]$, increments 0.1) and **S** and **T** ($R_{ST} = d[O_4{:}H_4] - d[N_1{:}H_4]) + d[N_2{:}H_3] - d[O_4{:}H_3]$, increments 0.2 Å). The initial parts of the calculated potential energy surfaces for this step were very different at the two levels of theory (see Figure 5). The lowest energy path on the AM1-CHARMM22 surface indicates an initial breaking of the lactam bond followed by protonation of the resulting negatively charged thiazolidine ring. However, from a biochemical point of view, a mechanism involving a stable structure with a negatively charged thiazolidine ring is very unlikely and is not supported by the higher level calculations.

Indeed, in contrast to the AM1-CHARMM surface, the B3LYP-corrected surface (Figure 5b) shows a diagonal lowest energy path with a single barrier, which indicates that the second acylation step, like the first, also has a concerted character. The cleavage of the β-lactam bond is accompanied by the protonation of the released nitrogen by Ser130 in a concerted reaction mechanism. In the approximate transition state ([q4;st3], see Figure 6), the breaking bond is stretched to 1.93 Å and the first moving proton is nearly equidistant between the oxygen of Ser130 and the accepting nitrogen (O_4-H_4, 1.2 Å and N_1-H_4, 1.34 Å). The oxygen of Ser130 forms a short hydrogen bond with Lys73 in the transition state, with the proton still bonded to the Lys73 nitrogen, as indicated by a N_2-H_3 distance of 1.02 Å, which is comparable to the equilibrium bond length. This shows that the second proton transfer (**T**) has not begun

(58) Jensen, F. Semiempirical Methods. *Introduction to computational chemistry*; Wiley: West Sussex, 1999; pp 81−96.
(59) Dkhissi, A.; Adamowicz, L.; Maes, G. *J. Phys. Chem. A* **2000**, *104*, 2112−2119.
(60) Loszynski, M.; Rusisnka-Roszak, D.; Mack, H.-G. *J. Phys. Chem. A* **1998**, *102*, 2899.
(61) Hayashi, T.; Mukamel, S. *J. Phys. Chem. A* **2003**, *107*, 9113−9131.
(62) Morpurgo, S.; Brahimi, M.; Bossa, M.; Morpurgo, G. O. *Phys. Chem. Chem. Phys.* **2000**, *2*, 2707−2713.

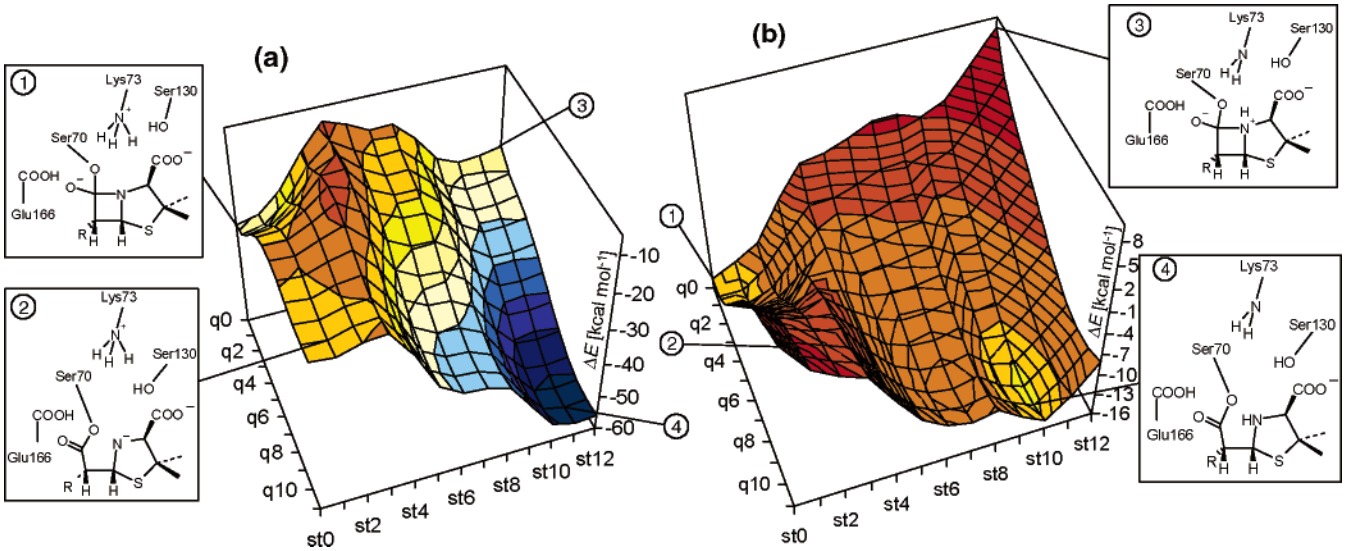

Figure 5. QM/MM potential energy surfaces for the reaction coordinates R_Q and R_{ST}. (a) AM1-CHARMM22 energies; (b) B3LYP/6-31G+(d)//AM1-CHARMM22-energies. (1) is the tetrahedral intermediate; (2) and (3) are unstable structures; and (4) is the acylenzyme (ester) intermediate.

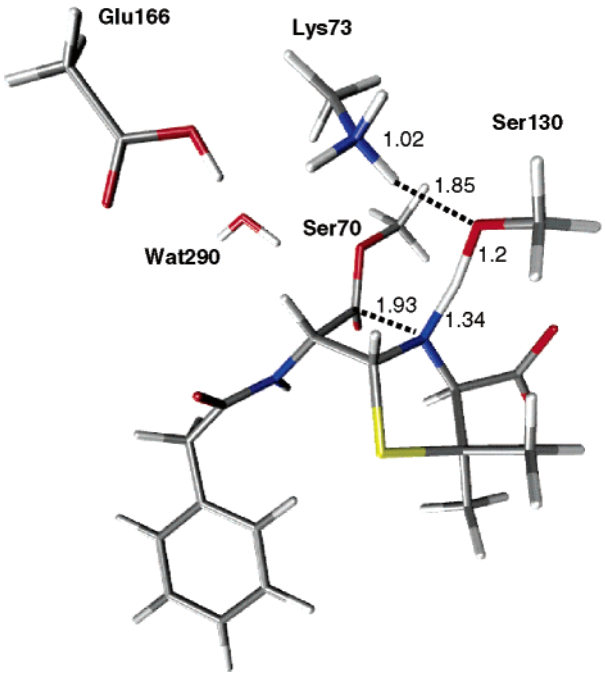

Figure 6. Transition state structure for the second acylation step (TS II), showing QM atoms only (B3LYP/6-31G+(d)//AM1-CHARMM22; point [q4;st3] on the surface shown in Figure 5). Some important distances are shown in angstroms.

at the transition state. A shallow energy minimum can be identified when the first proton transfer (**S**) is finished, and the subsequent "barrier" to the proton transfer from Ly73 to Ser130 (**T**) is calculated to be only 0.5 kcal mol^{-1}. This small barrier would probably disappear if zero-point energy effects were included. Therefore, the two proton transfers, although not absolutely synchronous, are strongly coupled at the level of theory used here. The barrier for the second acylation step was calculated to be 7.1 kcal mol^{-1} relative to the tetrahedral intermediate at the B3LYP/6-31G+(d)//AM1-CHARMM22 level and is lower than the barrier of the first reaction step.

At this stage of the reaction, Lys73 is left neutral and Glu166 remains protonated; therefore, the last step to complete the

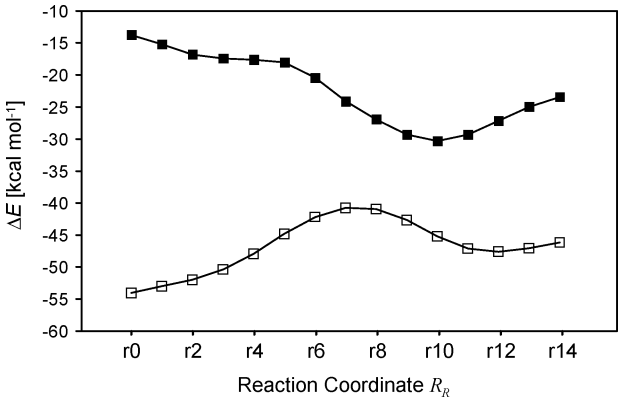

Figure 7. QM/MM energy profiles for proton transfer from Glu166 to Lys73 (see Scheme 2, **R**). Open boxes are AM1-CHARMM22 energies; filled boxes are B3LYP/6-31G+(d)//AM1-CHARMM22 energies (relative to the Michaelis complex).

acylation, with the formation of the acylenzyme, is a proton transfer from Glu166 to Lys73 (step **R**, see Scheme 2). This step was modeled with a single reaction coordinate (R_R = d[O_3:H_2] − d[N_2:H_2], increment 0.2 Å) starting from the intermediate of the previous step ((4) in Figure 5a). The energy profiles are plotted in Figure 7. AM1-CHARMM22 gave an endothermic profile for protonation of the Lys73 amino group of about 6.5 kcal mol^{-1}. In contrast, the B3LYP/6-31G+(d)//AM1-CHARMM22-profile reveals the expected exothermic character with an energy decrease of 16.5 kcal mol^{-1}. It is well known that AM1 often fails on energy balances of reactions in which the number of ions change, for example, in the calculation of basicities/acidities.[63] We have confirmed by gas-phase calculations that AM1 overestimates the stability of neutral acetic acid and methylamine (representing Glu166 and Lys73) relative to the corresponding ionized states by about 13 kcal mol^{-1} in comparison to B3LYP/6-31G+(d) results.[22] A similar effect is also responsible for the large energy change in the AM1-CHARMM22 surface of the previous step, when Ser130 is protonated by Lys73, by which both residues become neutral.

(63) Lewars, E. Semiempirical Calculations. *Computational Chemistry*; Kluwer Academic Publishers: Dordrecht, 2003; pp 339−382.

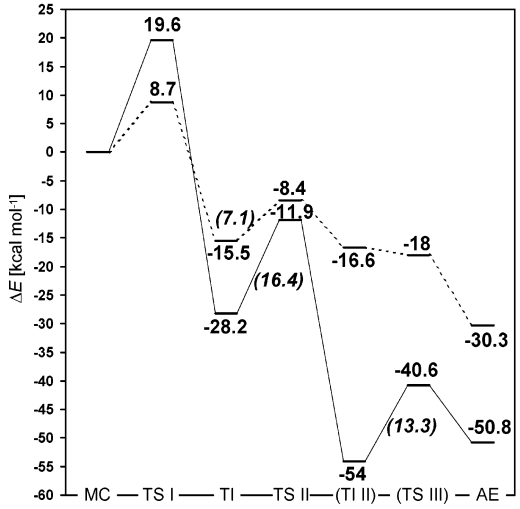

Figure 8. QM/MM energy profiles for the proposed acylation mechanism by class A β-lactamases (energies are given relative to the Michaelis complex (MC)). Solid line shows the AM1-CHARMM22 profile; dashed line shows B3LYP/6-31G+(d)//AM1-CHARMM22 profile. Energies are given for the transition state of formation of the tetrahedral intermediate (TS I), for the tetrahedral intermediate (TI), for the transition state of the second acylation step (TS II), and for the acylenzyme (AE). Energies are also given for (TI II) and (TS III), which are identified as stationary structures only at the AM1-CHARMM22 level (see text). Activation energies are given in parentheses.

A consequence of the erroneously high AM1 stability of the intermediate ((4) in Figure 5a) is the prediction of a stepwise mechanism by AM1-CHARMM22 for the subsequent reaction step (**R**), instead of a more concerted one (as indicated by the B3LYP corrected data). This artificial stability is also the reason it was not possible to calculate reliable surfaces based on AM1-CHARMM22 energies when transfer (**R**) was included in either of the previous reaction coordinates (R_Q, R_{ST}). These results emphasize the importance of the higher level energy calculations for this enzyme reaction.

The driving force of the second step of the acylation is the formation of the acylenzyme ester, which is significantly more stable than the tetrahedral intermediate (by 15 kcal mol^{-1} according to the B3LYP/6-31G+(d)//AM1-CHARMM22 results). Cleavage of the β-lactam bond and protonation of the thiazolidine ring and the related proton transfers are mandatory processes for that reaction. The proton transfer from Glu166 to Lys73 does not have a barrier: it is very likely to be concerted with the other reaction steps (**Q**, **S**, and **T**) as discussed above. An alternative pathway for the protonation of Lys73 involving a second water molecule as a proton shuttle has been suggested by Lamotte-Brasseur et al.[26] This mechanism has not been investigated here and cannot be excluded. However, the mechanism we find here does appear to be reasonable.

The full energy profile for the acylation at both levels is shown in Figure 8. The first reaction step, the formation of the tetrahedral intermediate, is likely to be rate-determining, because for that step the highest overall barrier was found on the basis of the results at both levels of theory. From the experimentally observed k_{cat},[25,64−66] the activation energy for cleavage of benzylpenicillin by TEM1 can be estimated (by transition state theory[67]) to be between 12.7 and 13.7 kcal mol^{-1}.[25,68−70] The calculated barriers of the first reaction step are in reasonably good agreement with the experimental data. The AM1-CHARMM22 barrier (19.6 kcal mol^{-1}) is overestimated, as expected. The B3LYP corrected barrier (8.7 kcal mol^{-1}) is lower and reasonably consistent with experiments. This supports the modeled mechanism based on Glu166 as the general base in acylation. The barrier for the second reaction step is lower than for the first, and the transition state for this later step is lower in energy than the substrate complex. The overall energy for the whole acylation reaction decreases by around 30 kcal mol^{-1} (B3LYP/6-31G+(d)//AM1-CHARMM22) and indicates a highly exothermic overall profile.

3. Amino Acid Decomposition Analysis. The decomposition analysis was performed for three important structures of the acylation reaction taken from the AM1-CHARMM22 surfaces. The Michaelis substrate complex was chosen as the reference structure. The results of the analysis for the transition state of the rate-determining first step ([x7;yz9]), and for the tetrahedral intermediate ([x17;yz19]), are given relative to the Michaelis complex. The energetic effects of individual amino acids on the AM1-CHARMM22 QM/MM interaction energies, indicating stabilizing or destabilizing effects, are plotted in Figure 9 as a function of the center of mass distance of a particular residue from the reaction center. Important residues are marked by an arrow. The influence of a particular amino acid can be deduced from the profiles directly through the observation of an energy increase (i.e., a stabilizing effect) or an energy decrease (destabilizing effect) relative to the Michaelis complex after its removal in the course of the decomposition. The interaction energies were calculated at the AM1-CHARMM22 QM/MM level and consist of the electrostatic QM/MM energy and the van der Waals interaction energy. This method gives a good description of interactions between atoms of the MM-region and atoms of the QM-region.[35,46,71]

Both the tetrahedral intermediate and the transition state are significantly stabilized by the enzyme relative to the substrate complex. The analysis shows that the tetrahedral intermediate is stabilized even more effectively by the enzyme environment (45 kcal mol^{-1}) than is the transition state (16 kcal mol^{-1}). It is clear that stabilization of the tetrahedral intermediate is central to the enzyme's function. The same interactions also stabilize the transition state, reducing the barrier to reaction. This is also a consequence of the analogous electronic character of the transition state and intermediate, which is shown by the Mulliken charges calculated here and was also found in a previous QM model study.[11] The contributions of individual residues to this stabilization are discussed below.

Met69, Ser70, Gly236, and Ala237. β-Lactamases have developed a special feature to stabilize charged tetrahedral geometries of the substrate formed during nucleophilic attack, called the "oxyanion hole", similar to that found in serine

(64) Fisher, J.; Belasco, J. G.; Khosla, S.; Knowles, J. R. *Biochemistry* **1980**, *19*, 2895−2900.
(65) Dalbadie-McFarland, G.; Neitzel, J. J.; Richards, J. H. *Biochemistry* **1986**, *25*, 332−338.
(66) Page, M. I. *Curr. Pharm. Des.* **1999**, *5*, 895−913.
(67) Garcia-Viloca, M.; Gao, J.; Karplus, M.; Truhlar, D. G. *Science* **2004**, *303*, 186−195.
(68) Fisher, J.; Belasco, J. G.; Khosla, S.; Knowles, J. R. *Biochemistry* **1980**, *19*, 2895−2900.
(69) Dalbadie-McFarland, G.; Neitzel, J. J.; Richards, J. H. *Biochemistry* **1986**, *25*, 332−338.
(70) Page, M. I. *Curr. Pharm. Des.* **1999**, *5*, 895−913.
(71) Garcia-Viloca, M.; Truhlar, D. G.; Gao, J. *J. Mol. Biol.* **2003**, *327*, 549−560.

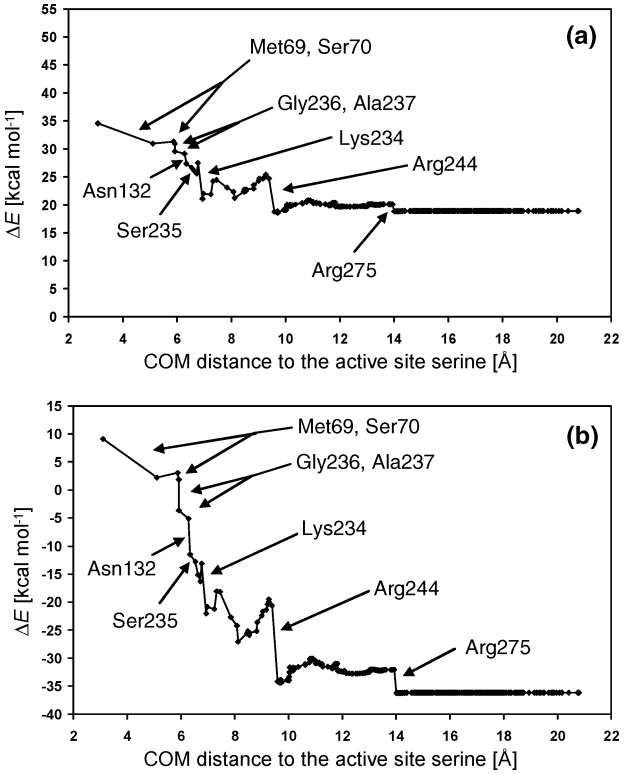

Figure 9. Amino acid decomposition analysis showing the energy contribution of every single MM-residue (ΔE = AM1-CHARMM22 interaction energy of residues whose center of mass distance (COM) is less than the corresponding value on the abscissa). Stabilization, relative to the substrate complex, is indicated when ΔE decreases; destabilization is indicated when ΔE increases. Plot a shows the result for the transition state (TS I). Plot b corresponds to the tetrahedral intermediate. Energies are given relative to the Michaelis complex and plotted against the center of mass (COM) distance of the particular amino acid to the reaction center.

proteases. The oxyanion hole in TEM1 β-lactamase is formed by the NH-groups of two peptide bonds (between Met69 and Ser70 and between Gly236 and Ala237). The backbone amide hydrogens of these bonds interact with the carbonyl oxygen of the β-lactam bond (see Figure 10). These interactions become increasingly stabilizing as the nucleophilic attack proceeds: they stabilize the transition state for the formation of the tetrahedral intermediate by 5.9 kcal mol^{-1}, and the tetrahedral intermediate by 15.2 kcal mol^{-1}. This stabilization increases with the magnitude of the charge of the oxygen (see Table 1; O_1). In the Michaelis complex, this oxygen is bound in the oxyanion hole (see Figure 10). As a consequence of the butterfly-like geometry of the bicyclus of benzylpenicillin, the β-lactam oxygen and nitrogen cannot form mesomeric structures (the nitrogen is sp^3-hybridized). The oxygen is ketone-like, rather than amide-like, and its negative charge is consequently relatively small (-0.39 as compared to, e.g., -0.55 for the amide oxygen of the side chain (see Table 1; atom O_2)). In the transition state, the geometry of the carbonyl group has changed away from the planar conformation, and the charge of the oxygen is increased (-0.47). At the tetrahedral intermediate, the charge of the former carbonyl oxygen is largest (-0.72) and so, consequently, is the stabilizing effect of the oxyanion hole. The stabilizing effect can be observed also through the change in the hydrogen-bond lengths. The more the charge of the oxygen increases, the shorter the hydrogen bonds become (see Figure 10).

The calculated stabilization of the transition state and of the tetrahedral intermediate are in good agreement with the results of a small model QM study of the TEM1 oxyanion hole, where the stabilizing effects for the transition state and the tetrahedral intermediate were 5 and 12 kcal mol^{-1} with RHF/6-31+G(d), and 4 and 14 kcal mol^{-1} using B3LYP/6-31+G(d).[11] These ab initio results are similar to the QM/MM findings, giving a good indication that these vital interactions are modeled well by the QM/MM method used here.

Asn132. Asparagine 132 is a highly conserved residue among class A β-lactamases. An important function of Asn132 is donation of a hydrogen bond from the NH2 of its side chain to the peptidic side chain which is present in almost all substrates, and which is crucial for positioning and binding in the active site (see Figure 11).[72] Analysis of interaction energies (see Figure 9) indicates that Asn132 also has an important stabilizing role in the reaction. This effect is strongest for the tetrahedral intermediate (6.4 kcal mol^{-1}), whereas the transition state for the formation of the tetrahedral intermediate is stabilized by 1.8 kcal mol^{-1} relative to the Michaelis substrate complex.

The interaction of Asn132 with the substrate's peptidic side chain is unlikely to be responsible for these differences in stabilization. Neither the charge of the bound carbonyl oxygen (see Table 1; atom O_2), nor the length of the hydrogen bond, change significantly during the acylation reaction. We found that the stabilization is based on another, mechanistically important interaction that is not related to a direct contact with the substrate. In the Michaelis complex, the side-chain oxygen of Asn132 accepts a hydrogen bond from Lys73 with a length of 1.9 Å (see Figure 11). The positive charge of Lys73 is stabilized additionally through hydrogen bonds to Ser70 and Ser130 and a salt bridge with Glu166 (see Figure 11). It is obvious that the main stabilization of the positive charge of Lys73 is from the interaction with the carboxylate group of Glu166. This group acts as the general base and is protonated during the acylation. This means that its interaction with and stabilizing influence on Lys73 are lost and the hydrogen bond with Asn132 becomes more essential for the stabilization of Lys73 as the reaction proceeds. These effects can be observed by means of the lengths of the hydrogen bonds involved, and the charges of the atoms. In the transition state, the accepting oxygen of Glu166 is partly protonated, and its charge is reduced (see Table 1, charge of O_3 is -0.48). The length of the hydrogen bond of Glu166 with Lys73 is increased by about 0.4 Å, and the hydrogen bond of Lys73 to Asn132 is stronger and shorter by 0.12 Å (see Figure 11). Glu166 is protonated in the tetrahedral intermediate, and the salt bridge to Lys73 has been lost. The H-bond to Asn132 is shorter (1.7 Å) in the tetrahedral intermediate than at any other stage of the reaction. Asn132 stabilizes the tetrahedral intermediate most (6.4 kcal mol^{-1}). The other hydrogen-bond partners of Lys73 cannot provide the same stabilization: Ser130 is further away ($N_2H_3-O_4$ distance of 2.14 Å), and the hydroxylic oxygen of Ser70 is transformed to an ester oxygen at the tetrahedral intermediate. Asn132 is therefore a very important amino acid for stabilizing the positive charge of Lys73 in the active site. These results are in good agreement with N132A-mutation experiments of Jacob et al.[73]

(72) Auterhoff, H.; Knabe, J.; Höltje, H.-D. β-Lactam-Antibiotika. *Lehrbuch der Pharmazeutischen Chemie*; WVG: Stuttgart, 1999; pp 675−686.
(73) Jacob, F.; Joris, B.; Lepage, S.; Dusart, J.; Frére, J.-M. *Biochem. J.* **1990**, *271*, 399−406.

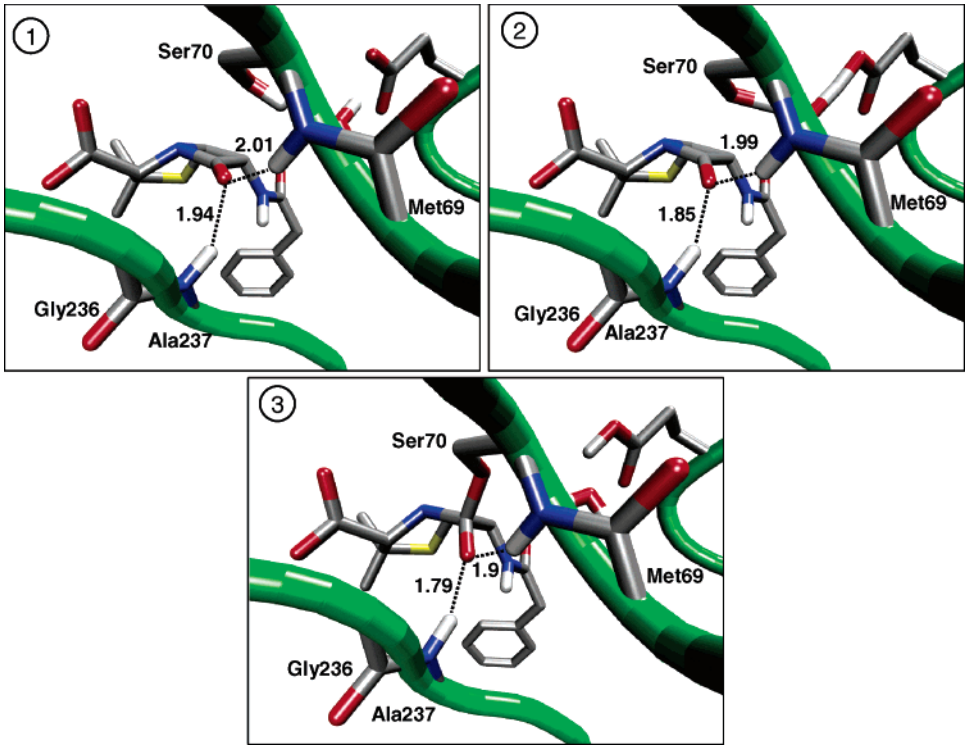

Figure 10. QM/MM optimized structures (AM1-CHARMM22) of the oxyanion hole during tetrahedral intermediate formation, showing important hydrogen bonds (with distances in Å) between the backbone hydrogens of Ser70, Ala237, and the carbonyl oxygen. (1) is the Michaelis complex; (2) is the transition state; and (3) is the tetrahedral intermediate.

Table 1. Mulliken Charges (Calculated at the AM1-CHARMM22 QM/MM Level) of Some Important QM-Atoms for Different Structures of the Acylation Reaction (AM1-CHARMM22 Structures)

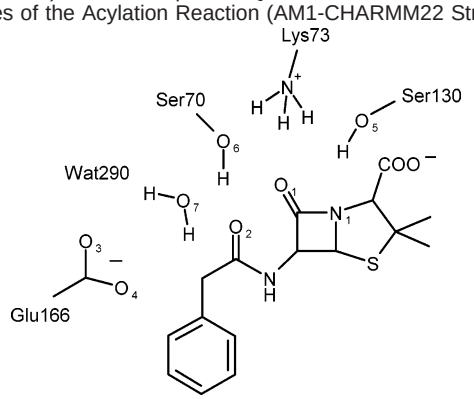

atom	Michaelis complex	transition state	tetrahedral intermediate
O_1	−0.39	−0.47	−0.72
O_2	−0.51	−0.54	−0.57
O_3	−0.64	−0.48	−0.33
O_4	−0.67	−0.54	−0.47
O_5	−0.40	−0.42	−0.45
O_6	−0.42	−0.57	−0.39
O_7	−0.55	−0.63	−0.47
N_1	−0.25	−0.26	−0.31

They concluded from their results that Asn132 is more important for catalysis than for the formation of the Michaelis complex. Our calculations help to explain these experimental findings for Asn132. Asn132 appears at least partly responsible for the exothermic character of the acylation and potentially vital for the efficiency of antibiotic breakdown. This additional important function of Asn132 appears to be in good agreement with its conservation in class A β-lactamases.

Lys234, Ser235, Arg244, and Arg275. These four residues will be discussed together because their contribution to the stabilization comes from the compensation of the same geometrical and energetic changes within the QM-region during acylation. This stabilization is larger for the tetrahedral intermediate than for the transition state. The effects are larger than those discussed above, because of the ionic character of these interactions, except Ser235, which has a minor contribution to the stabilization of 0.5 kcal mol^{-1} for the transition state and 2.4 kcal mol^{-1} for the tetrahedral intermediate. Lys234, Arg244, and Arg275 together stabilize the tetrahedral intermediate by 29 kcal mol^{-1}, and the transition state by 14 kcal mol^{-1} relative to the substrate complex (see Figure 9).

The stabilization is a result of the electronic changes within the QM-atoms during the formation of the intermediate. The positively charged residues are located at the opposite side of the active site from Glu166 (see Figure 12). As a consequence of the protonation of Glu166 in acylation, its negative charge is transferred toward that side of the active site (mainly to the carbonyl oxygen of the β-lactam bond; see Table 1, O_1). Arg244, Lys234, and Ser235 form an "anchor cavity" for the carboxylate side chain of the substrate. The more negative charge moves toward this cavity, the more the stabilizing effect of these residues increases. Some negative charge has built up in this part of the substrate in the transition state, but it is most evident in the tetrahedral intermediate (see Table 1), which is consequently stabilized most by these residues.

In addition to the movement of charge, the change in the geometry must be considered. The substrate carbonyl carbon changes from a planar sp^2 to a tetrahedral sp^3 conformation as a result of the nucleophilic attack. During the reaction, the C−O dipole changes its orientation toward Arg275 (and Arg244,

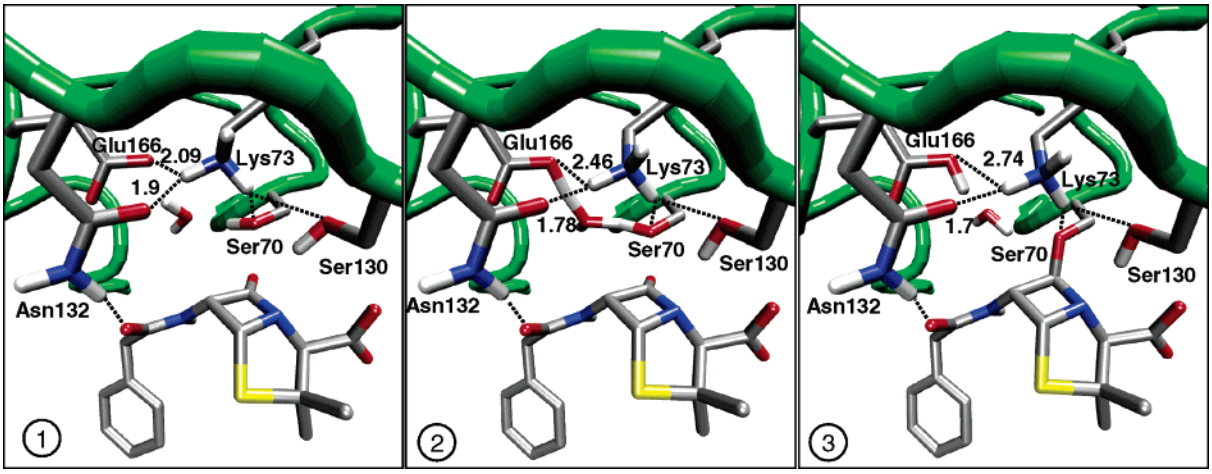

Figure 11. QM/MM optimized structures (AM1-CHARMM22) of the active site in the acylation reaction, showing hydrogen bonds (with distances in angstroms) of Lys73 and other important active site residues. (1) is the Michaelis complex; (2) is the transition state; and (3) is the tetrahedral intermediate.

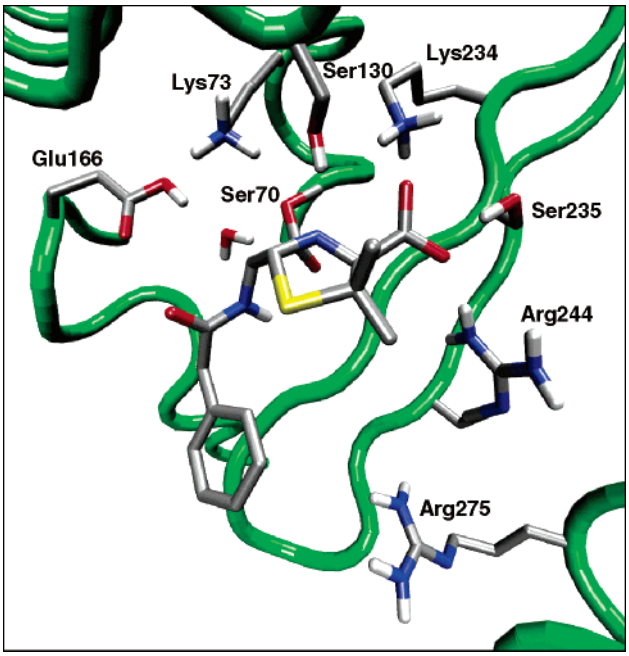

Figure 12. QM/MM optimized structure of the tetrahedral intermediate in the TEM1 β-lactamase, showing some important residues.

which is also roughly in that direction). This change is most apparent in the tetrahedral intermediate. This suggests that the reason for the observed improved electrostatic interactions during the reaction are not only due to the increased negative charge on the oxygen in the transition state and tetrahedral intermediate, but also to the changed orientation of the former β-lactam oxygen carbonyl group dipole. As the decomposition analysis shows, the active site of the enzyme is well organized to provide this stabilization. The oxyanion hole, Asn132, positively charged residues close to the active site, and the anchor cavity are important for catalysis: they stabilize the transition state and the tetrahedral intermediate by electrostatic interactions.

Lys73. The strongly conserved amino acid Lys73 has been suggested to be the active site base due to the observation that K73-mutants have decreased acylation rates.[25,32] Because Lys73 was included in the QM region, its influence was not included in the QM/MM decomposition analysis. Nevertheless, its main functions can be deduced from the results, which explain the decreased acylation rate in K73 mutants. Our analysis reconciles the experimental findings with a mechanism in which Glu166 acts as the base. Lys73 contacts every important catalytic residue (Ser70, Ser130, Asn132, Glu166, and the catalytic water molecule) and so is central to the hydrogen-bonding network of the active site. Another important role of Lys73 is its function as a proton relay station for the proton transfer from Glu166 to the β-lactam nitrogen for the second step of the acylation reaction (see Scheme 2 and discussion of that process). The conversion of the tetrahedral intermediate to the acylenzyme would probably be crucially impaired without Lys73, in accord with the experimentally observed reduced acylation rates. Furthermore, Lys73 may play some catalytic role in the formation of the tetrahedral intermediate: a function of Lys73 in stabilizing the transition state of that first step of acylation was proposed in previous investigations.[12] This is likely because of its position in the active site close to the oxygen of Ser70 ($\sim$2.8 Å), which is more negatively charged in the transition state than in the Michaelis complex (see Table 1; O_6). This suggests an improved interaction with the positively charged Lys73. However, the calculation of mutant effects involving Lys73 turned out to be highly sensitive to structural changes within the active site and indicates that further investigations are necessary to determine its role in transition state stabilization in the formation of the tetrahedral intermediate.

A central goal in research on β-lactam antibiotics is the development of new antibiotics with greater resistance to inactivation by lactamases. The results presented here suggest that the stability of β-lactam antibiotics against class A β-lactamases could potentially be improved through alterations to give them the ability to interact with the Ser70 activation machinery. PBPs lack an equivalent of Glu166 (or a similar residue to act as a general base), a crucial difference from class A β-lactamases. Inhibition of Ser70 activation could therefore provide stability against β-lactamases without losing antibiotic potency. For example, structural modifications of β-lactams that replace the catalytic water were successful and show the efficacy of that strategy.[74] Other modifications can be envisaged and could be a fruitful new area of development: for example, compounds that interact with Asn170 to inactivate the important

(74) Matagne, A.; Lamotte-Brasseur, J.; Dive, G.; Knox, J. R.; Frère, J.-M. *Biochem. J.* **1993**, *293*, 607−611.

hydrogen bond to the catalytic water, or compounds which address both functionalities of the Asn132 side chain to destabilize transition states and intermediates, could be useful directions to explore in structure-based drug design.

Conclusions

The most plausible mechanism for the complete first step of the breakdown of β-lactam antibiotics by class A β-lactamases, the acylation reaction, has been investigated here by QM/MM calculations for the first time, with the physiological protonation state of Lys73. The results are consistent with the available experimental data and provide new insight into the detailed mechanism of this important reaction. Key groups and interactions within the active site have been identified, and detailed insight has been obtained about their role in the reaction. Some of these new insights may give valuable directions in the development of new antibiotics. Modeling of the acylation reaction shows the nucleophile, Ser70, is activated by deprotonation indirectly by Glu166, which abstracts a proton from an intervening water molecule, which in turn deprotonates Ser70. The results thus support a symmetric nucleophile activation mechanism, where Glu166 acts as the general base in both acylation and deacylation steps. Calculations have been performed with high-level corrections and generally support mechanistic conclusions from a lower level QM/MM modeling study.[12] The high-level (hybrid density functional) method, however, was found to be necessary here to give reliable energetics. Indeed, the calculated activation barrier is in good agreement with experimental data. The calculations reveal that the enzyme active site is well organized for efficient breakdown of lactam antibiotics, with key groups (including a catalytic water molecule) optimally positioned for the various reaction processes. Little overall structural change occurs in the proposed mechanism.

The mechanism proposed in the present work consists of two main reaction steps. In the first step, Glu166 abstracts a proton from Ser70 via a conserved water as a proton relay station. This deprotonation activates the serine for nucleophilic attack on the β-lactam antibiotic. Analysis of the energy profiles and potential energy surfaces reveals that formation of the tetrahedral intermediate follows a concerted mechanism in which the two proton transfers (from Ser70 to the water and from the water to the general base, Glu166) happen in the same step as the nucleophilic attack of Ser70 on the β-lactam carbonyl group. The transition state for this concerted step is the highest energy point for the whole acylation reaction at the applied levels of theory. The transition state structure is "dominated" by the proton transfer to Ser70. This suggests that the easier is the deprotonation of Ser70 (in the presence of a particular β-lactam antibiotic), the lower is the barrier for acylation and the less stable the antibiotic would be to class A β-lactamases.

The calculations also identify a likely mechanism for the second reaction step, the formation of the acylenzyme intermediate, involving several proton transfers. Upon cleavage of the β-lactam bond, the β-lactam nitrogen is protonated by Ser130. Ser130 is then immediately reprotonated (indirectly) by Glu166, with Lys73 as a proton shuttle residue. This step was found to happen concertedly. The apparently synchronous breaking of the lactam bond and protonation of the lactam nitrogen by Ser130 is accompanied by the slightly delayed proton transfers from Lys73 to Ser130 and from Glu166 to Lys73 (reprotonation of Ser130). The barrier of the whole second reaction step was found to be lower than that for the first step at both levels of theory, suggesting that the first step (i.e., formation of the tetrahedral intermediate) is the rate-determining reaction step in acylation.

An amino acid decomposition analysis of the first step of the reaction (formation of the tetrahedral intermediate) showed the enormous impact of the enzyme environment on the reaction energetics, by stabilization of key structures. In particular, the rearrangement of charges during acylation (e.g., the movement of the negative charge toward atoms in a more central position in the active site) and the accompanying changes of key geometric features (such as the change of the β-lactam carbonyl carbon from sp^2 to sp^3 hybridization) are complemented very well by the enzyme active site. Both the transition state and (particularly) the tetrahedral intermediate were found to be significantly stabilized by the enzyme relative to the bound substrate. Many residues close to the active site contribute by electrostatic interactions. Residues forming the oxyanion hole (Met69, Ser70, Gly236, and Ala 237), and others including those forming the anchor cavity for the substrate carboxylate group (Lys234, Ser235, Arg244, and Arg275), were identified as being important in this stabilization. A new, potentially vital function of the conserved residue Asn132 in catalysis (the stabilization of the positively charged Lys73) was revealed, in addition to its role in binding the substrate through an interaction with the peptidic side chain of β-lactam compounds. Effects such as these demonstrate the necessity of including the protein environment in investigations of β-lactamase acylation. They are crucial determinants of the energetics of the reaction that are not accounted for in studies on small model systems.[11,5,75]

The results suggest routes for the modification of β-lactam antibiotics that could increase their stability against class A β-lactamases. In particular, modifications that impair the deprotonation mechanism of Ser70 could be promising. This activation machinery is different from the actual targets of β-lactams, the PBPs, which lack key residues of the class A β-lactamase active site, such as the general base Glu166. Therefore, the sensitivity of PBPs to such modified β-lactam antibiotics should not be affected. The present results and conclusions demonstrate how QM/MM calculations of enzyme reactions can help to elucidate their mechanisms, provide unique insights into catalytic features of the enzyme active site, and may contribute to structure-based drug design.

Acknowledgment. J.C.H. thanks the Royal Society for a visiting fellowship (2004/R2-EU). A.J.M. thanks BBSRC, EPSRC, The Wolfson Trust, The Royal Society, and the IBM Life Sciences Outreach Program for support. L.R. thanks the EU Quality of Life FP5 program for a Marie Curie Individual Fellowship under contract number QLRI-CT-1999-51244.

Supporting Information Available: AM1, B3LYP/6-311+G(d,p), and HF/6-311+G(d,p) optimized geometries of β-lactam models. This material is available free of charge via the Internet at http://pubs.acs.org.

JA044210D

(75) Alvarez-Idaboy, J. R.; González-Jonte, R.; Hernández-Laguna, A.; Smeyers, Y. G. *J. Mol. Struct. (THEOCHEM)* **2000**, *504*, 13−28.
(76) Humphrey, W.; Dalke, A.; Schulten, K. *J. Mol. Graphics* **1996**, *14*, 33−38.